Pol. J. Environ. Stud. Vol. 30, No. 1 (2021), 369-384
DOI: *10.15244/pjoes/120773* ONLINE PUBLICATION DATE: 2020-08-22

Original Research

Applicability of a Three-Stage Hybrid Model by Employing a Two-Stage Signal Decomposition Approach and a Deep Learning Methodology for Runoff Forecasting at Swat River Catchment, Pakistan

Muhammad Sibtain[1]*, Xianshan Li[1], Muhammad Imran Azam[2], Hassan Bashir[3]

[1]Laboratory for Operation and Control of Cascaded Hydropower Station, China Three Gorges University,
[2]College of Hydraulic & Environmental Engineering, China Three Gorges University, Yichang 44302, P. R. China
[3]College of Environmental Science and Engineering, Hunan University, Changsha 410082, P. R. China

Received: 22 January 2020
Accepted: 18 April 2020

Abstract

The optimal management of hydropower resources is highly dependent on accurate and reliable hydrological runoff forecasting. The development of a suitable runoff-forecasting model is a challenging task due to the complex and nonlinear nature of runoff. To meet the challenge, this study proposed a three-stage novel hybrid model namely IVG (ICEEMDAN-VMD-GRU), by coupling gated recurrent unit (GRU) with a two-stage signal decomposition methodology, combining improved complete ensemble empirical decomposition with additive noise (ICEEMDAN) and variational mode decomposition (VMD), to forecast the monthly runoff of SWAT river, Pakistan. ICEEMDAN decomposed the runoff time series into subcomponents, and VMD performed further decomposition of the high-frequency component obtained by ICEEMDAN decomposition. Afterward, the GRU network was employed to the decomposed subcomponents for forecasting purposes. The performance of the IVG model was compared with other hybrid models including, ICEEMDAN-VMD-SVM (support vector machine), ICEEMDAN-GRU, VMD-GRU, ICEEMDAN-SVM, VMD-SVM; and standalone models including GRU and SVM by utilizing statistical indices. Experimental results proved that the IVG model outperformed other models in terms of accuracy and error reduction, which indicates the feasibility of the IVG model to analyze the nonlinear features of runoff time series and for runoff forecasting with applicability for future planning and management of water resources.

Keywords: runoff forecasting, time series, hybrid model, signal decomposition, machine learning

*e-mail: sibtain92@ctgu.edu.cn

Introduction

Natural runoff is the primary source of water and plays a vital role in irrigation, conservation of the environment, and socioeconomic growth [1]. Optimum distribution and utilization of water resources are getting more focus due to the insecurity of hydro resources [2]. Reliable and accurate forecasting of runoff and weather are important factors in decision making regarding reservoir management and operation, allocation of water supply, and drought and flood management [3-5]. However, devising an efficient model for runoff and rainfall forecasting poses a challenge, since the runoff and rainfall depend on nonlinear factors including precipitation, uneven flow, topography, anthropic activities, and evaporation [6, 7]. Owing to its importance, hydrological forecasting is now a popular study area, and researchers have applied many forecasting techniques to predict runoff forecasting in the past decades [8]. There are two types of runoff forecasting models: process-driven and data-driven. Process-driven models focus on the physical processes of the hydrological cycle and employ empirical formulas. This approach requires a correct description of the hydrological process [8, 9]. Forecasting is done through data-driven models with the aid of intelligent algorithms and mathematical methods by exploiting statistical properties of unknown hydrological black-box in watersheds or river catchments [8]. The data-driven approach uses historical runoff data and climate factors for future forecasting of runoff data. The data-driven approaches are gaining popularity for accurate forecasting due to their rapid growth, fewer information requirements compared to the process-driven models, and the increasing computational power [10]. SVM, fussy (rule-based) systems, artificial neural network (ANN), and model trees (MT) are the most commonly used data-driven approaches for hydrological forecasting [11].

Deep learning based machine learning (ML) is a particular area of interest nowadays in runoff forecasting with various models being used for runoff modeling. Compared to the statistical models, ML models are applicable and overcome the constraints for the non-stationary and non-linear runoff time series, with better accuracy and performance [12, 13]. ML models such as SVM and ANN represent the latest area of research for forecasting runoff time series [14]. The study in [15-17] provides a comprehensive review of ML models for runoff forecasting and modeling.

Hydrological systems have been widely studied by employing artificial intelligence techniques [18]. The robustness and the efficiency of the SVM algorithm, allow the applicability of SVM for runoff forecasting studies. Furthermore, the promising results and the excellent simplification ability of SVM for runoff forecasting, make this technique superior compared to the other ML models [19-22]. Moreover, recurrent neural networks (RNNs) have a long history in the field of hydrology with applications for rainfall-runoff modeling since the 1990s [23, 24]. The study conducted in 2004 compared RNN with ANN for monthly streamflow forecasting and analyzed that RNN outperformed feed-forward ANN. Long short term memory (LSTM) overcomes the issue associated with traditional RNN of learning long-term dependencies within hydrological catchments, which may play a significant role in the hydrological processes [25]. Gated recurrent unit (GRU) like LSTM is also a variant of RNN and allows GRU to discard useless information and maintain useful information in dynamic sequence data, with additional benefits of retaining all advantages of RNN [26].

The standalone models sometimes omit useful information when applied alone, therefore, the hybrid models have been proposed to apply for the forecasting of the hydrological time series [27]. These hybrid models have the ability to deal with the intricate problems more efficiently [28]. To overcome the inadequacies of the data-driven models and for more reliable and accurate forecasting, hybrid data-driven models combine the decomposition techniques with artificial intelligence techniques [29, 30].

Hybrid ML models improve the accuracy of forecasting with efficient data management [31, 32]. Furthermore, these models also provide the benefits of automated and well-timed management and performance assessment of the ensemble algorithms [33]. The study in [34] and [35], overviews the hybrid ML models for runoff-rainfall forecasting.

Multilevel periods exist in the hydrological times series, which exhibit changes in the time domain. Numerous decomposition techniques have been introduced to separate the different time scales having non-linear and non-stationary variables in the hydrological times series that also provide support for runoff forecasting and system analysis [36-38]. The data gathered at regular intervals constitute a time series, while the time series analysis is performed by employing statistical methods [39].

The decomposition methods for time series are feasible to improve the working of ML models used for rainfall-runoff and runoff modeling. The ML models forecast the sub-components obtained through the decomposition of the observed time series, and thereby improve the forecasting results [12]. Wavelet transform (WT), Empirical Mode Decomposition (EMD), Ensemble Empirical Mode Decomposition (EEMD) are widely used for decomposition of hydrological runoff time series. But they face problems like producing some false harmonic signals as in the case of WT [40], mode mixing of intrinsic mode functions (IMFs) and the orthogonality effect faced by EMD [41, 42], complexity and residual noise issue of EEMD [43]. Therefore, CEEMDAN was proposed, which is superior to EEMD and resolves many issues, as suffered by EEMD. However, CEEMDAN also fails to remove the residual noise present in the modes, and the early decomposition

stages have some spurious modes with delay in the appearance of signal information [44].

Improved CEEMDAN is an advanced version of CEEMDAN and obtains IMFs having less residual noise with more physical importance [45]. ICEEMDAN utilizes the observed signal for IMF sifting to get rid of the issues faced by EMD and its variants [46]. Despite having good results for signal decomposition [46], the ICEEMDAN does not find appreciable implementations for runoff forecasting.

Unlike EMD based techniques, VMD decomposes the observed time series into sub-components and updates them [47]. VMD has an outstanding performance in frequency search and separation, with robust noise and sampling properties [48]. The VMD is comparatively a new technique for hydrological application [12], and relatively a few studies exist regarding the application of VMD for runoff forecasting.

Therefore, this study proposes a three-stage hybrid model IVG based on ICEEMDAN, VMD and GRU, and its applicability to forecast the monthly runoff at Swat River, Pakistan. Pakistan is an agricultural country with an economy that is based on the surface water [49]. The accurate runoff forecasting is important since the difference between the water requirement and the precipitation adversely affects crop production [50]. Natural disasters, including floods and droughts, are serious threats for Pakistan [51]. The economic development of the country suffers from major floods, which the country experiences almost every three years [52]. The devastating flood of 2010 in the country forecast the occurrence of more extreme events in the future [53]. Consequently, the accurate drought forecasting is essential to lessen the adverse effects of droughts [54].

The above facts highlight the significance, and need for accurate runoff forecasting for Pakistan, therefore, this study considers the runoff forecasting with the main objectives as given below:

Owing to the importance of runoff for Pakistan, this study considers the runoff forecasting with the main objectives as given below:

(1) The development of ML and signal decomposition based hybrid model by taking into account the monthly hydrological runoff data of the Swat River;
(2) Applicability of the hybrid model for the runoff forecasting; and
(3) Verifying the performance and accuracy of the proposed model by comparing results with the similar models developed to forecast the monthly runoff.

The rest of the paper is arranged as follows. Section 2 describes the modeling techniques and the proposed approach. The results and discussion are presented in section 3, while section 4 concludes this study. This study will be useful for forecasting and planning purposes and will provide new directions in the field of hydrology.

Materials and Methods

Proposed Hybrid Modelling

The non-stationary and nonlinear characteristics of runoff [55, 56] lead to the undesirable performance of many forecasting models and poor generalization, and also affects the accurate knowledge of data variations [57]. Therefore, this paper proposes a three-stage hybrid model to analyze the dynamic behavior of hydrological time series for accurate runoff forecasting, by coupling a ML model with the signal decomposition techniques.

The main steps can be explained as given below:

Step 1: This step applies the Pearson correlation coefficient method to the observed runoff data to determine the appropriate input variable.

Step 2: The observed runoff time series is decomposed through ICEEMDAN technique into subcomponents (IMFs) having a different frequency.

Step 3: The VMD decomposes the high pass component (IMF1) generated by ICEEMDAN into the subcomponents.

Step 4: GRU network was applied to construct a forecasting model by taking the observed runoff series,

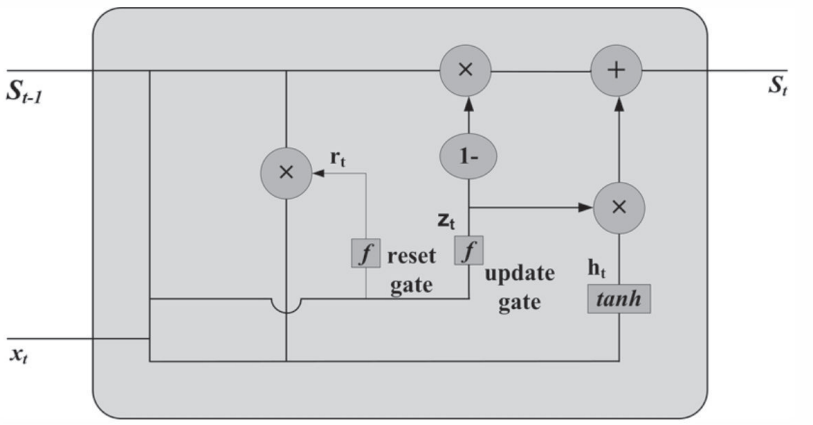

Fig. 1. The basic model of GRU.

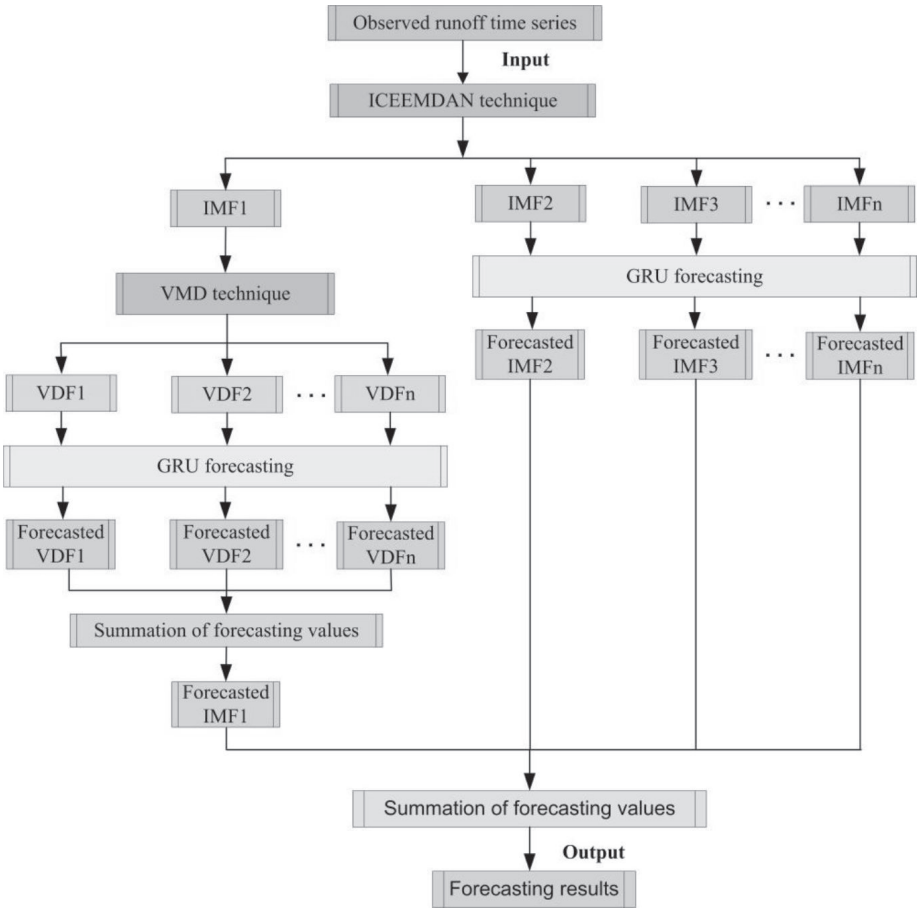

Fig. 2. A flowchart of the proposed hybrid IVG model.

its selected lagged values with strong correlations, and subcomponents produced by the decomposition techniques. The basic model of GRU is given in Fig. 1 [58].

Step 5: This step reconstructs the predicted results of step 4 for final forecasting.

Step 6: Finally, the statistical performance metrics (root mean square error (RMSE), mean absolute error (MAE), Nash-Sutcliffe efficiency coefficient (NSE), and the coefficient of determination (R^2) evaluate the results in the training and testing periods.

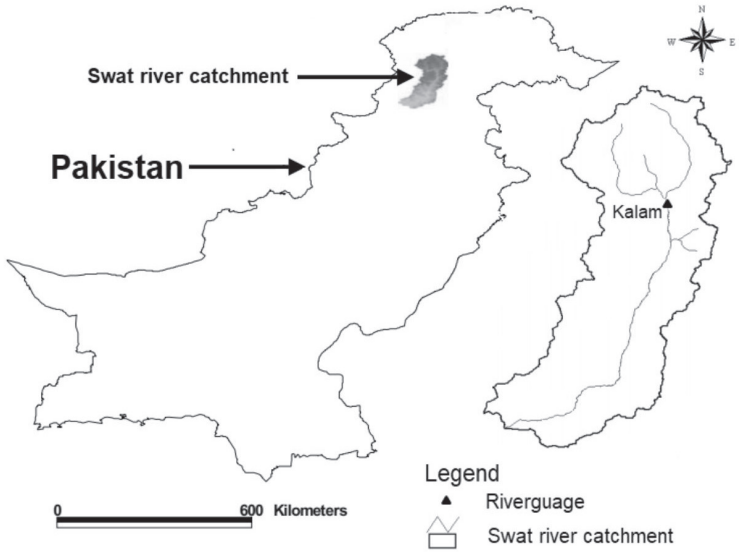

Fig. 3. The location of Swat river catchment in Pakistan.

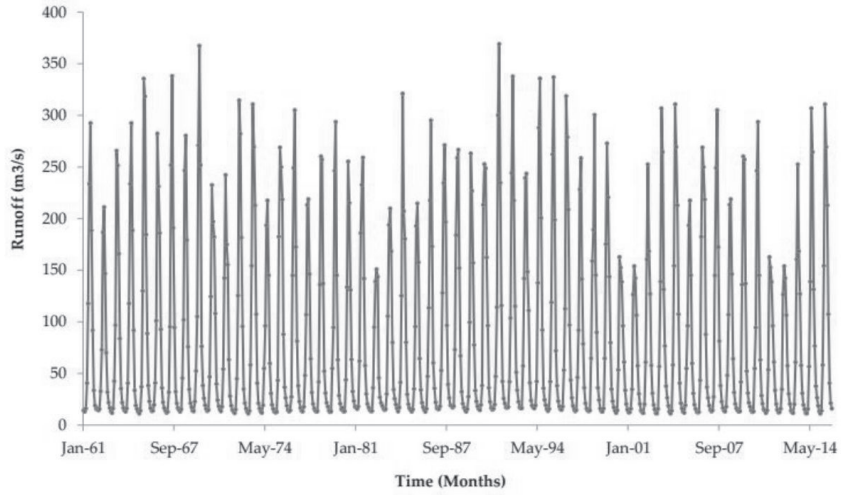

Fig. 4. The monthly runoff of Swat River at Kalam.

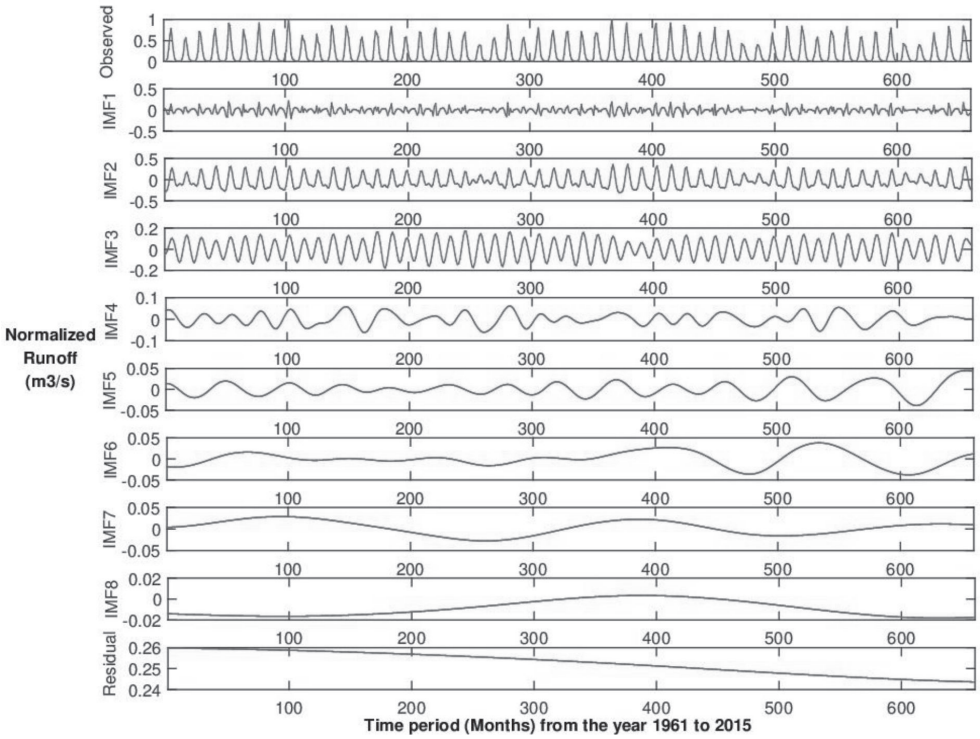

Fig. 5. Decomposition of the runoff time series using ICEEMDAN.

The flow diagram representing the main steps of the proposed methodology is given in Fig. 2.

Case Study

This study considers the runoff data of Swat river catchment located within longitude 70°59' east to 72°47' east and latitude of 34°00' north to 35°56' north in the northern region of Khyber-Pakhtunkhwa Province, Pakistan [59]. The Swat river is a perennial river with origin from Hindukush mountains and streams up to Madyan through the Kalam valley and lower areas of Swat valley up to Chakdara. The river discharges into the Kabul River and has a total span of 240 km.

Table 1. The correlation coefficient between the input signal and the IMFs of ICEEMDAN.

IMF/Residual	IMF1	IMF2	IMF3	IMF4	IMF5	IMF6	IMF7	IMF8	Residual
Correlation coefficient	0.344	0.948	0.847	0.097	0.073	0.080	0.054	0.020	0.017

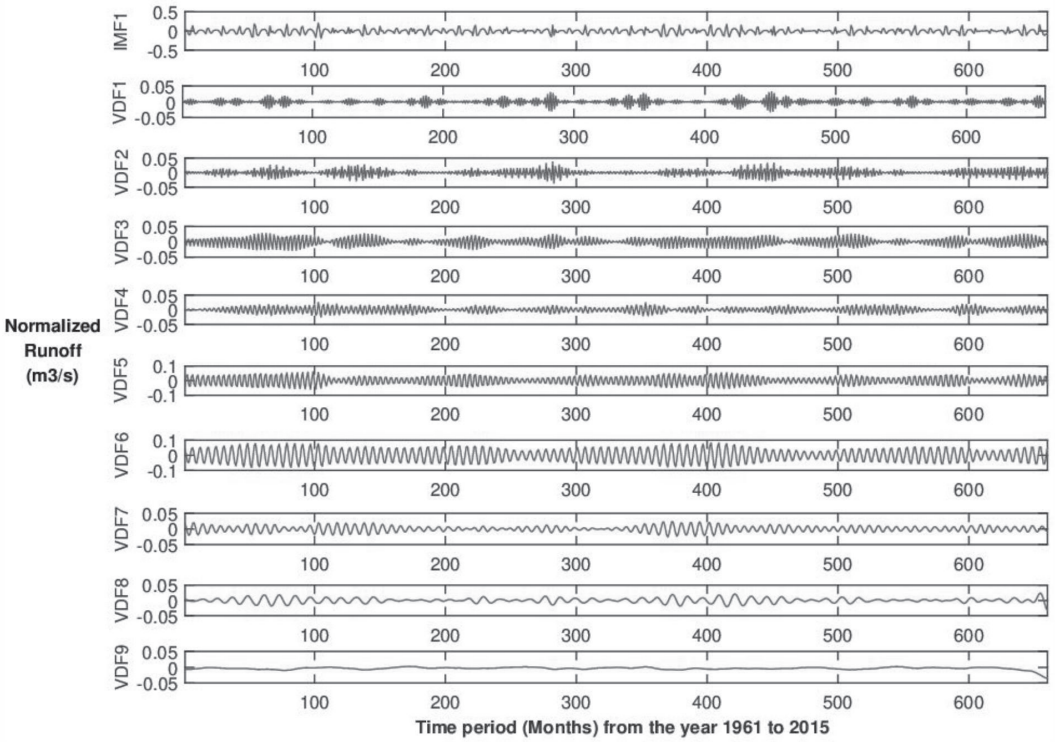

Fig. 6. VMD of IMF1 (obtained after ICEEMDAN).

The swat river serves for power generation, irrigation, and the natural habitat of birds and fishes. A huge hydropower potential exists in the Swat river basin, and the plans include the construction of numerous hydropower projects in the future [60]. These facts signify the importance of the Swat River for the future economic growth of the country [59]. The catchment area of the SWAT River is mostly rocky, with altitudes stretching from 360 m to 4,500 m approximately, from south to north. The location of the Swat River catchment in Pakistan is shown in Fig. 3.

Data Selection

The runoff data for the forecasting purpose was collected from Water and Power Development Authority (WAPDA), Pakistan. The monthly runoff data of the Swat River from 1961 to 2015, as shown in Fig. 4, was taken at Kalam hydrological station in the Swat river catchment.

Results and Discussion

Decomposition Results

ICEEMDAN technique is applied to decompose the runoff series into the eight independent IMFs and the Residual (Fig. 5). The de-noising of the observed runoff series is not necessary due to the good anti-noise properties of the CEEMDAN technique [43]. The IMF1 has a maximum amplitude, and the highest

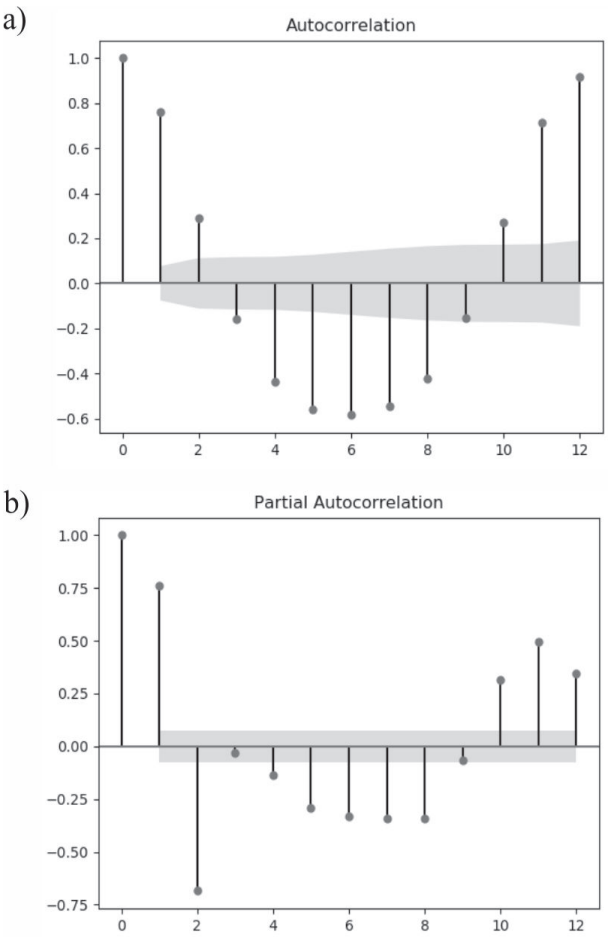

Fig. 7. The auto-correlation function a) and the partial autocorrelation function b).

Table 2. Inputs selection for different models.

Model	Inputs
GRU/SVM	X_t, X_{t-1}, X_{t-11}, X_{t-12}
ICEEMDAN-GRU/ICEEMDAN-SVM	X_{t-1}, X_{t-11}, X_{t-12}, IMF1-IMF8, r
VMD-GRU/VMD-SVM	X_{t-1}, X_{t-11}, X_{t-12}, VF1-VF9
IVG/ICEEMDAN-VMD-SVM	X_{t-1}, X_{t-11}, X_{t-12}, IMF2-IMF8, r, VDF1-VDF9

frequency, whereas, all the other IMFs (IMF2~IMF8) and the Residual (r) show a gradual reduction in the amplitude and frequency with an increase in the wavelength.

VMD performs a secondary decomposition of IMF1 due to the presence of high oscillatory contents in IMF1. The mode determination of the VMD technique requires careful consideration. The study in [6] utilizes a trial and error method to select mode, whereas the study in [61] employs correlation analysis for the mode determination in ensemble decomposition techniques. The present study also utilizes the Pearson correlation coefficient analysis of the intrinsic modes including the Residual produced by ICEEMDAN technique and the observed runoff series as provided in Table 1.

The IMF2 shows a strong correlation with the observed runoff series; therefore, based upon [61], the obtained value of mode determination is 9. The decomposition results of IMF1, obtained by employing VMD, are shown in Fig. 6.

VMD decomposed the IMF1 into nine modes from VDF1-VDF9, as shown in Fig. 6. Compared to the other decomposition techniques, VMD generates smoother intrinsic modes [62], which is also evident from the decomposition result of IMF1.

Input Selection and Model Development

Seven other models were also developed to compare the effectiveness of the proposed IVG model, including ICEEMDAN-VMD-SVM, ICEEMDAN-GRU, VMD-GRU, GRU, ICEEMDAN-SVM, VMD-SVM, and SVM. Pearson's correlation coefficient was applied to determine a suitable dataset and correlation between the variables. Pearson's correlation coefficient can deal with large datasets and has low complexity and strong generality, making it feasible for feature selection of the input dataset [63]. This method utilizes correlation indicators to determine the appropriate inputs and filters the inputs having scores greater than the threshold [64]. An autocorrelation function (ACF) and partial autocorrelation function (PACF) with twelve lags applied to the observed runoff series are shown in Fig. 7.

This study considers a threshold value of 0.5 for the correlation coefficient, and the runoff time series

Table 3. Parameters and hyperparameters selection.

Technique/Model	Parameters and hyperparameters
ICEEMDAN	Standard deviation of noise (Nstd): 0.2; Number of realizations allowed (NR): 500; Signal to noise ratio flag (SNRFlag): 2; Maximum number of sifting iterations allowed (MaxIter): 5000.
VMD	Moderate bandwidth constraint (Alpha): 2000; Number of modes (K): 9; Noise tolerance (tau): 0; Initialization of omegas (init): 1; Tolerance of convergence (tol): 1e-7.
SVR-based models	Kernel: Radial basis function (RBF); Regularization parameter (C): C ∈ [1.0, 2.0, 5.0, 8.0, 10.0, 15.0]; Sigma (σ): $\sigma \in$ [0.1, 0.05, 1, 2, 2.5, 3.5]; Epsilon : (ε) $\in \varepsilon$ [0.001, 0.01, 0.03, 0.05, 0.1, 0.15].
GRU-based models	Input layer: One; Size of first and second hidden layer: (64, 32), (128, 64); Number of training epochs: (50, 200); Learning rate (lr): lr ∈ 10^{-3}; Optimizer: RMSprop; Dropout rate: 0.2; Batch size: (30, 50); Output layer: One.

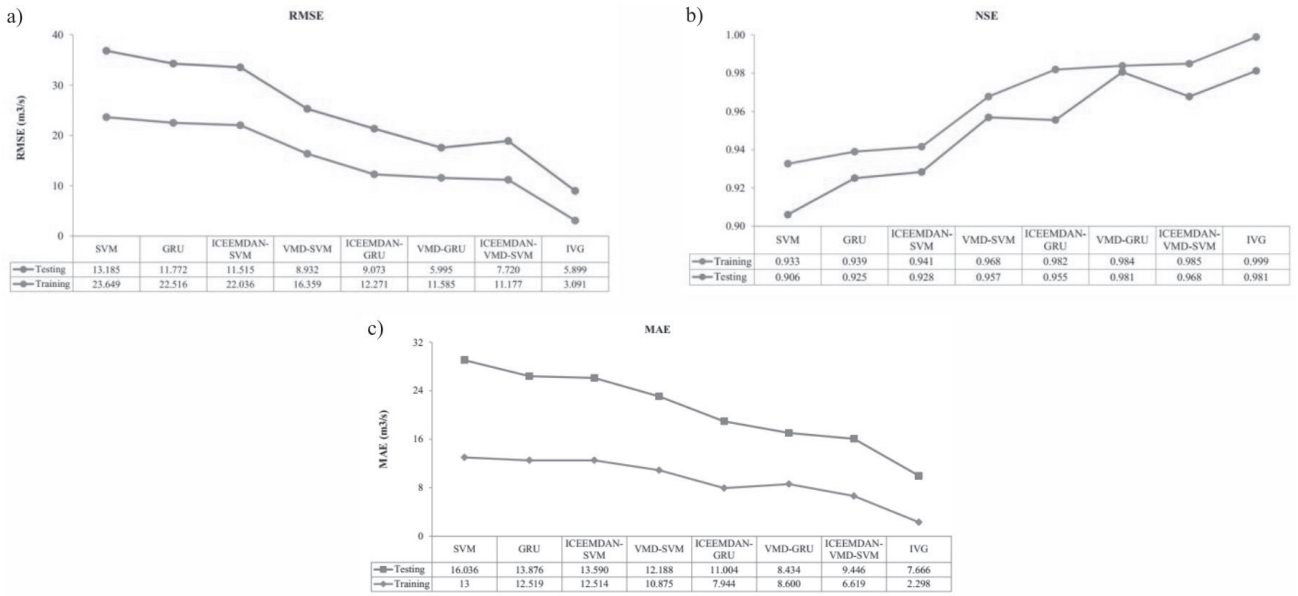

Fig. 8. Performance evaluation of models using statistical indices: a) RMSE, b) NSE, c) MAE.

having values greater than 0.5 were selected as input features of the forecasting model. As per Fig. 5 a), since the autocorrelation coefficient values at first, eleventh, and twelfth lag show values greater than 0.5, therefore, these values are selected as three lagged inputs for the input dataset. The other inputs include modes produced by ICEEMDAN and VMD. The detailed inputs for all models to predict a 1-month-ahead runoff (X_{t+1}) are provided in Table 2.

Where X_t, X_{t-1}, X_{t-11}, and X_{t-12} represent the runoff at the current time, first lag, eleventh lag, and twelfth lag, respectively, while IMF1-IMF8 and r represent IMFs and Residual produced by ICEEMDAN decomposition respectively. VF1-VF9 denotes intrinsic modes of VMD produced by the direct decomposition of runoff series; whereas, VDF1-VDF9 represent intrinsic modes of VMD produced by the decomposition of high-frequency component (IMF1) of ICEEMDAN decomposition. The first two models in Table 2 are the single forecasting models that are constructed using the observed runoff series, and the three lagged runoff series as inputs. The second two models are hybrid models based on ICEEMDAN technique and ML models with three lagged inputs and decomposed subseries by ICEEMDAN technique as their inputs. Similarly, the third two models are hybrid models based on VMD technique and ML models with three lagged inputs and decomposed subseries by VMD technique as their inputs. Finally, the last two models of Table 2 are the three-stage hybrid models with three lagged runoff series and decomposed subseries by ICEEMDAN and VMD techniques as their inputs.

The dataset for input to ML models is divided into training (approximately 80% of the whole dataset) and testing datasets (approximately 20% of the whole dataset). Neural networks require input features to be normalized to match the comparative significance of the inputs, and this study performs the task of normalization by employing the minmax scalar technique as given by Equation 20 [65]. Moreover, the normalized values are also used as an input to the decomposition techniques.

$$\widetilde{X} = \frac{X - \text{Min}\,(X)}{\text{Max}\,(X) - \text{Min}\,(X)}$$

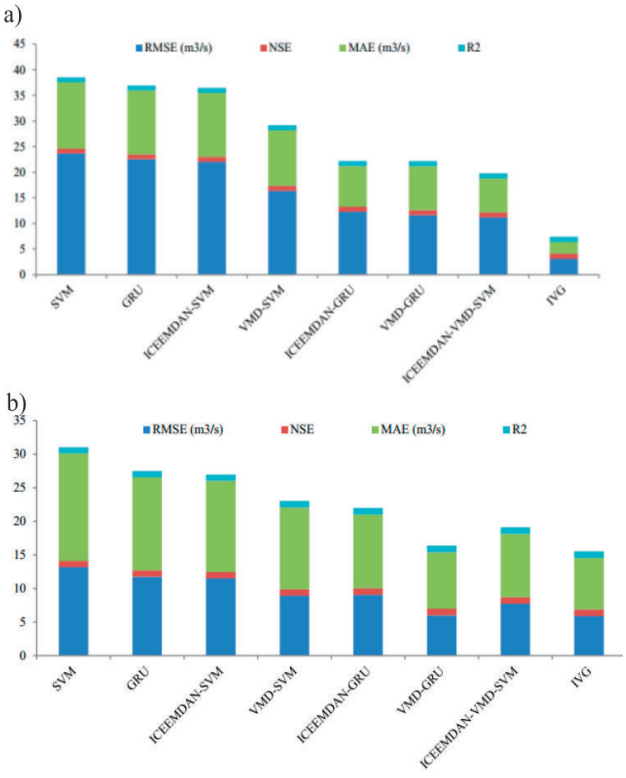

Fig. 9. Comparative analysis of models using performance indices. a) Training Period, b) Testing period.

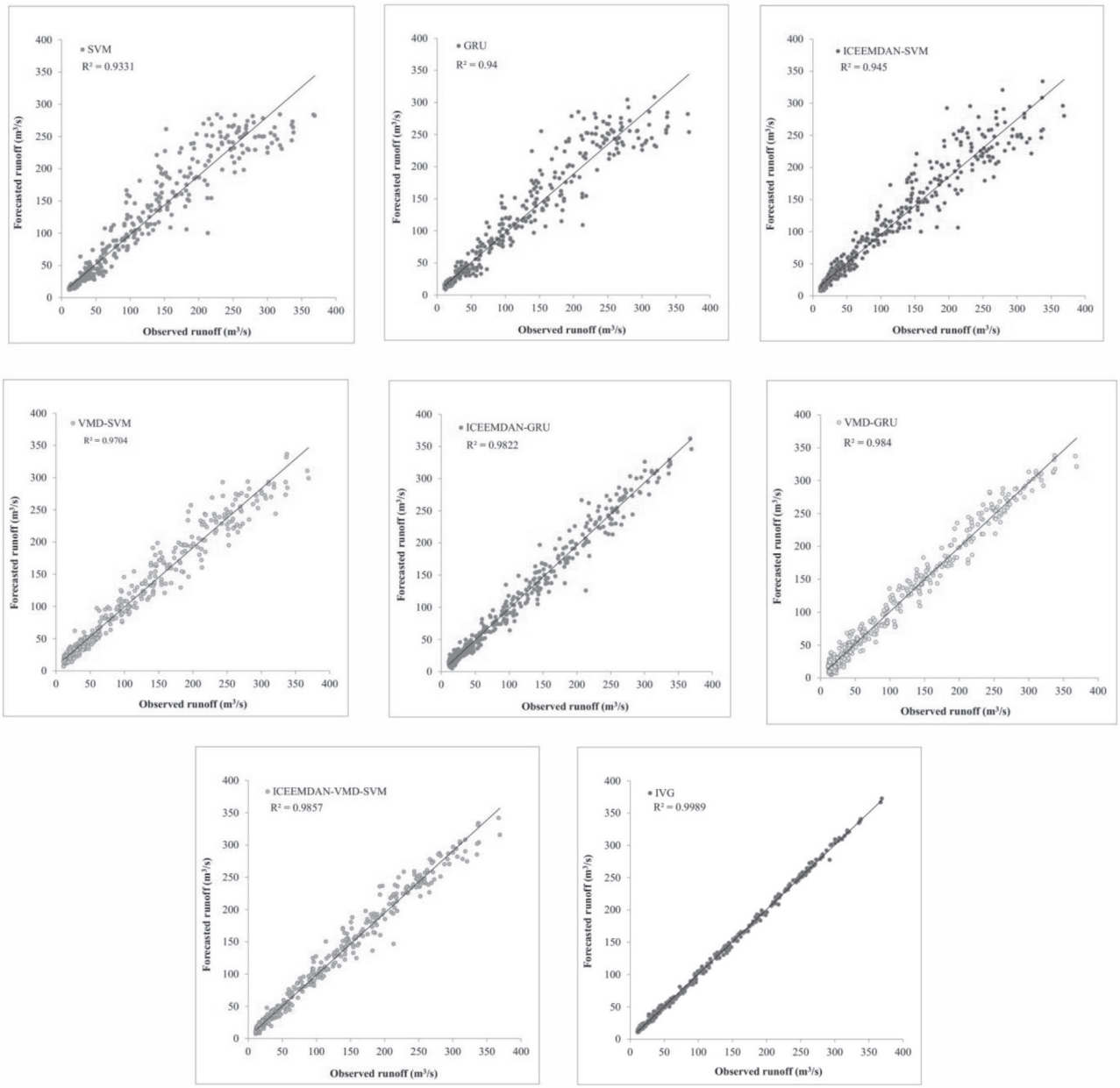

Fig. 10. Scatter plots of the observed and forecasted runoff during the training period.

Models Structure, Parameters and Hyperparameters

This study was performed by utilizing a 64-bit Windows 10 operating system, on a 3.70 GHz, Intel (R) Core i7-10510U CPU, with 16 GB RAM. The analysis was carried out in Matlab R2015a software, and PyCharm environment employing Python 3.6 programing language relying on Pandas and Numpy packages. The accurate determination of model parameters is important for hydrological forecasting to make a model behave closer to the real world [66]. Tensorflow based ML models are also used by many researchers [67]. Therefore, ML models were developed with Keras using Google Tensorflow backend. The detail of parameters and hyperparameters selection by the decomposition techniques and ML models is provided in Table 3.

The parameters of ICEEMDAN and VMD techniques are the same for all hybrid models. The RBF was taken as a kernel for SVR-based models, while the three parameters including the regularization parameter, epsilon and sigma were determined through the grid search approach by employing a ten-fold cross-validation. The RMSprop optimizer performs better in recurrent neural networks [68], therefore this study considers RMSprop as an optimizer for the GRU-based models, while the other hyperparameters of the GRU were selected after different trials and errors.

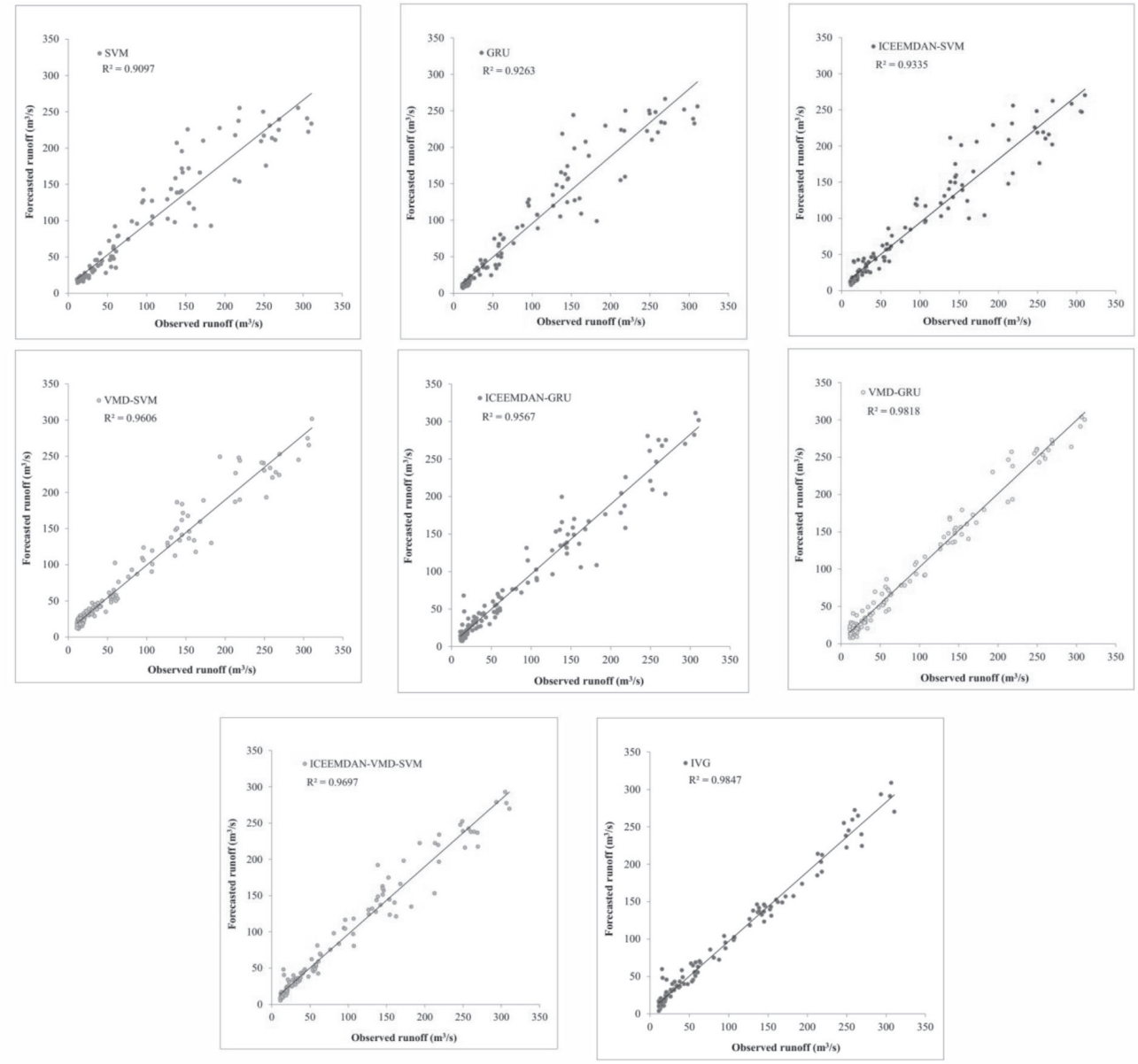

Fig. 11. Scatter plots of the observed and forecasted runoff during the testing period.

Forecasting Outcomes and Relative Analysis

The input datasets as per Table 2 were applied to the models for training and testing of data. The effectiveness of the IVG model was evaluated by comparing the results of the IVG model with the other seven models during the training and testing periods.

Fig. 8 and Fig. 9 shows the result of one month ahead forecasting by all models in the course of the training and testing periods by utilizing the statistical indexes. The highest error in terms of RMSE and MAE was recorded for SVM with values of 23.649 m^3/s, 13.185 m^3/s, and 13 m^3/s, 16.036 m^3/s, respectively during the training and testing periods. In terms of NSE, the IVG model shows the most accurate results during the training and testing period with values of 0.999 and 0.981, respectively, compared to all the other models.

As per the modeling results, the IVG model shows the lowest error values compared to the other hybrid and standalone models. Similarly, the VMD-based hybrid forecasting models reveal better performance for reducing errors than the ICEEMDAN-based hybrid forecasting models, which shows the effectiveness of the VMD technique in processing the runoff time series. Furthermore, the GRU model shows better error reduction results than the SVM-based models, which highlights the superiority of the GRU network over the SVM algorithm for runoff forecasting. The comparative analysis of models utilizing RMSE, NSE, MAE, and R^2 also presents the lowest error values for the IVG model during training and testing periods while the SVM model shows the poorest results, as shown in Fig. 9.

To elaborate on the superior performance of the IVG model for the runoff forecasting, a comparison of correlation between the observed and forecasted

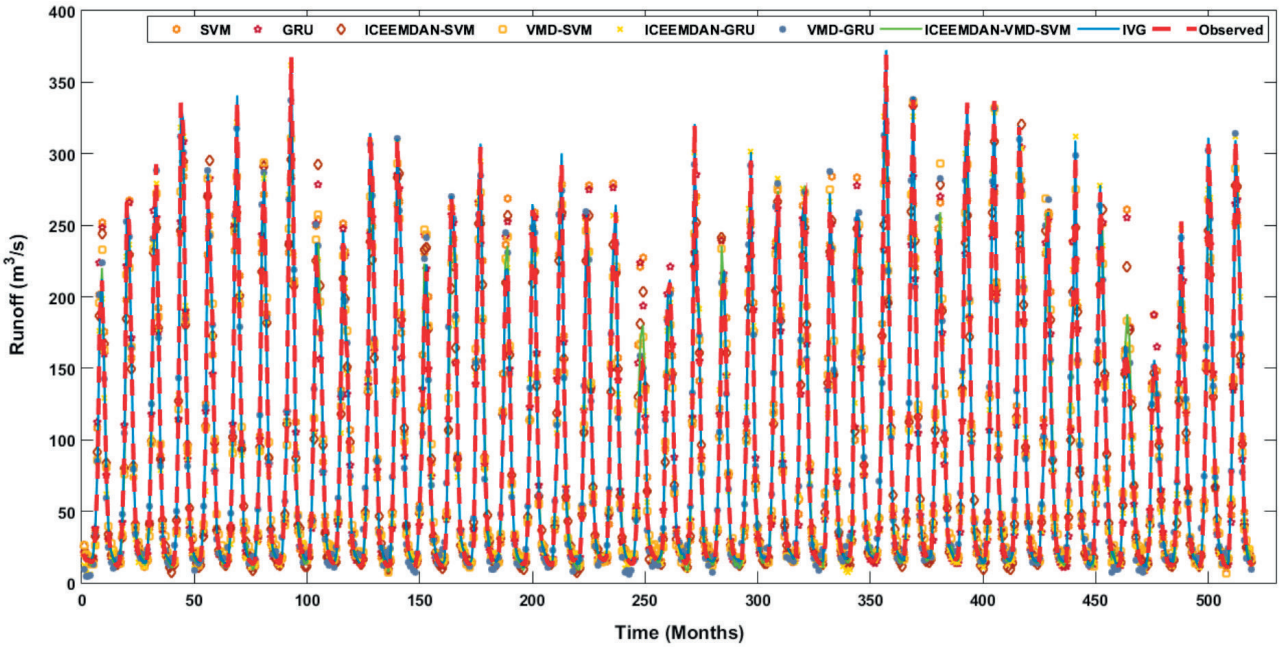

Fig. 12. Comparison of the observed and forecasted runoff during model training period using IVG and other models.

runoff for different models is provided in Fig. 10 and Fig. 11 using scatterplots. The analysis shows a stronger correlation between the observed and predicted monthly runoff in the case of the IVG hybrid model than the other models. Moreover, the other hybrid approaches also performed well in capturing the low and high runoff values than the standalone models. The observed and forecasted runoff during the training period shows more degree of agreement then the testing period.

The observed and the predicted runoffs for standalone models show lower correlation values than the hybrid models. However, in the case of hybrid combination, the performance of the standalone SVM and GRU models was significantly improved, which reflects the significance of the hybrid combinations.

The scatterplots of Fig. 10 and Fig. 11 reveals a closer linear agreement line near to the perfect line (1:1) for the IVG model compared to the other hybrid and standalone models. Moreover, the VMD-GRU hybrid model agrees more with the observed and forecasted runoff than the ICEEMDAN-VMD-SVM hybrid model during the testing period. The results of scatterplots

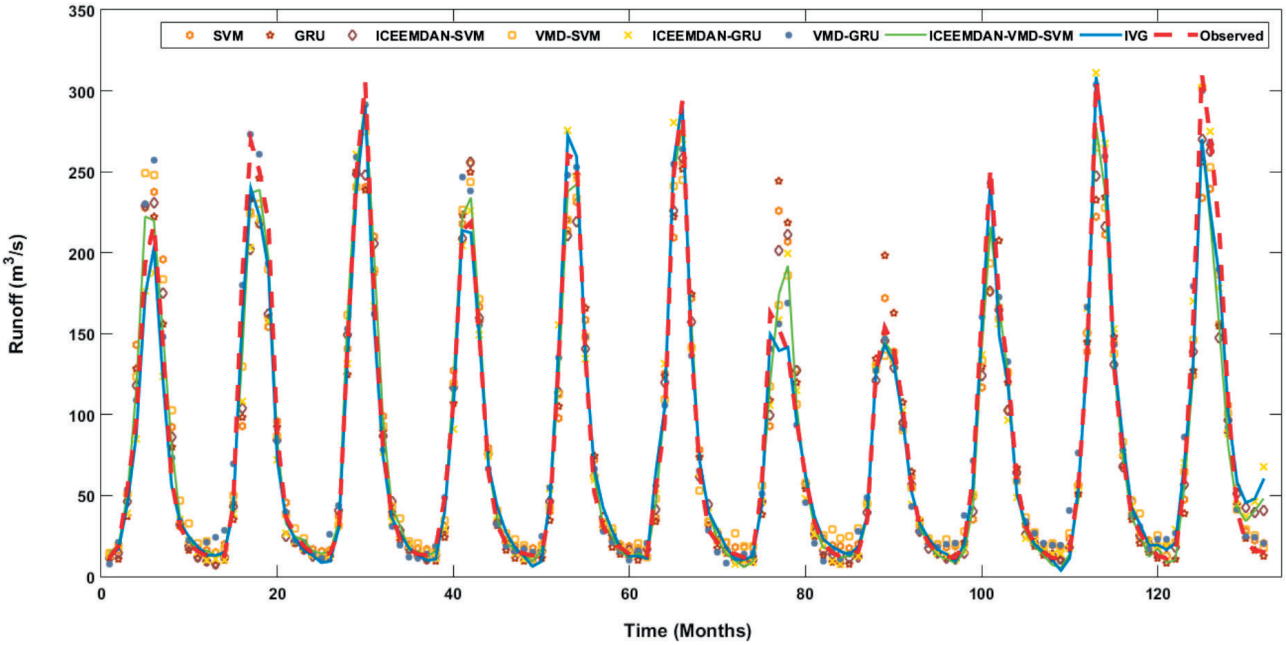

Fig. 13. Comparison of the observed and forecasted runoff during model testing period using IVG and other models.

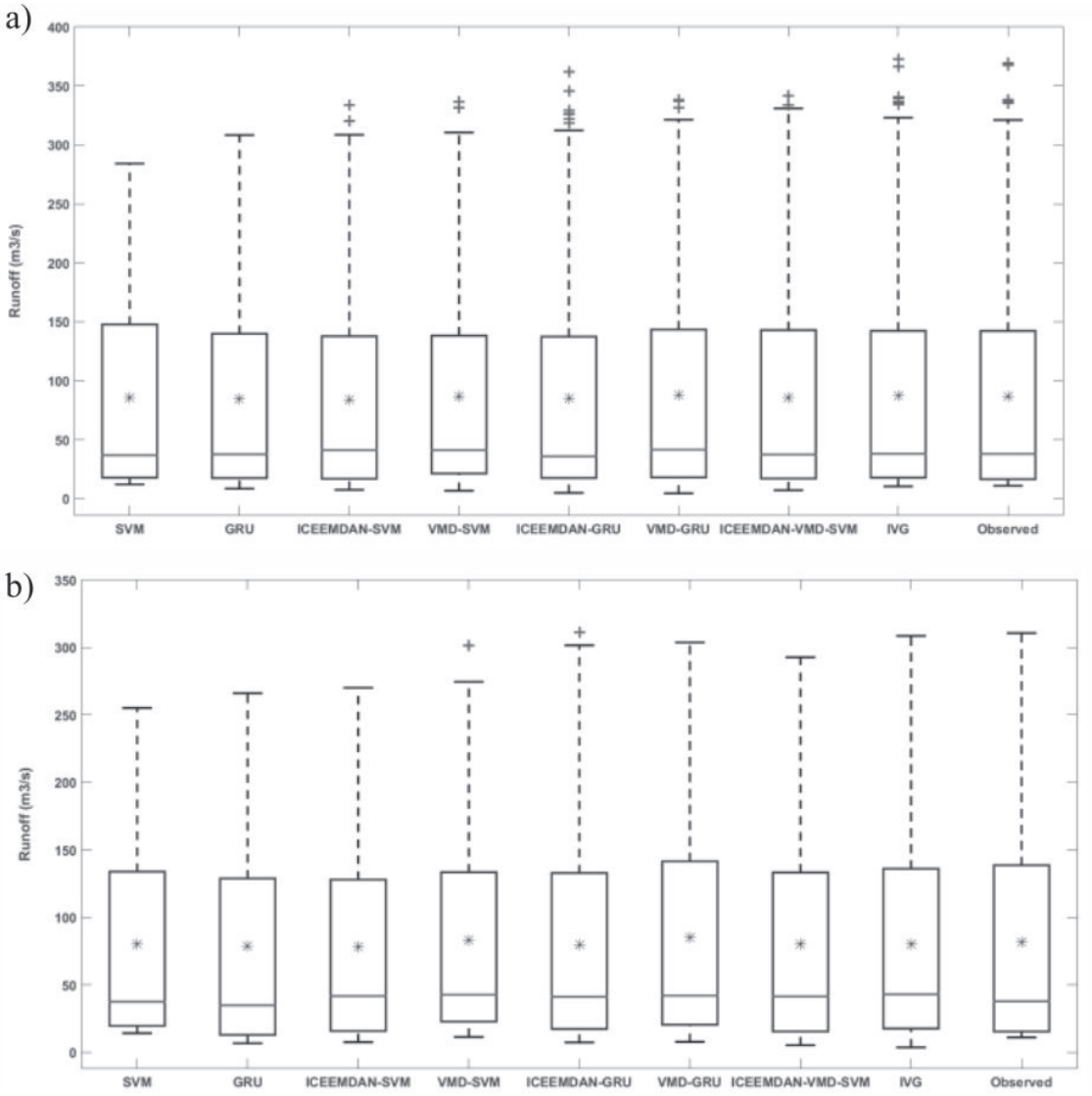

Fig. 14. Boxplots of the observed and forecasted runoff by different models.

reveal the suitability of ICEEMDAN, VMD and GRU for runoff forecasting, and feasibility of ICEEMDAN and VMD techniques in preprocessing the runoff data and forecasting monthly runoff.

Fig. 12 and Fig. 13 provide the comparison curves of the actual and forecasted runoff for all models during the model training and testing periods. The behavior of the IVG model is better and stable than all the other models, which indicates the superior aptness of the IVG model to study the nonlinear features of the runoff series.

The IVG model can mimic the runoff well than the other models in both training and testing phases, and overall the hybrid approaches perform better than the standalone models. The boxplots in Fig. 14 and Fig. 15 visually calculate the performance of models during the training and testing periods. Using quartiles, the boxplot shows the spread of observed and forecasted runoff with whiskers showing the changeability outside of the 25th and 75th percentiles.

The minimum value of runoff for the observed data is 11.012 m^3/s during the training period, while the IVG model has a minimum runoff value of 10.506 m^3/s that is closer to the observed runoff value than shown by all the other models. For example, the ICEEMDAN-VMD-SVM and VMD-GRU models minimum runoff values are 7.234 m^3/s and 4.553 m^3/s, respectively. Likewise, the maximum runoff value of the IVG model during the training period is 372.459 m^3/s, which again shows a closer value to the observed runoff value of 369.107m^3/s, while ICEEMDAN-VMD-SVM and VMD-GRU models show the runoff values of 341.682 m^3/s and 338.258 m^3/s, respectively.

The range of runoff shown by the IVG model during the testing period is 304.901 m^3/s, which is near to the observed runoff range of 299.536 m^3/s, while the ICEEMDAN-VMD-SVM model shows a range of 287.404 m^3/s. Furthermore, the SVM-based forecasting models show more skewness and dispersion than the GRU-based forecasting models. Moreover, the training

period provides more adroit forecasting than the testing period. The SVM and GRU standalone models reveal the poor performance compared to hybrid models in forecasting the monthly runoff by undervaluing the bulk of high runoff data.

The performance of the three-stage ICEEMDAN-VMD-SVM model is also better compared to the two-stage hybrid models (ICEEMDAN-SVM, VMD-SVM). However, the performance of the ICEEMDAN-VMD-SVM model in terms of accuracy and error reduction is inferior to the VMD-SVM hybrid model. The results reveal that the ML and decomposition-based ensemble models are superior to the individual ML models since the complex input signal is decomposed into simple-to-study sub-components by the decomposition approaches, which are promising to analyze and forecast.

All the hybrid models performed well in all simulations, although the runoff forecasting is a complex task. The results prove the findings of [69-71], according to which, it is practically difficult for a standalone model to forecast precisely the complex hydrological runoff process, due to the effects of the external factors. The superior results of the IVG model prove the viability of the IVG model, for the runoff forecasting and can provide a feasible reference, for the applicability of the IVG model to forecast similar tasks. The IVG model can identify the complicated nonlinear relation between the observed and the forecasted runoff data with the best performance and accuracy. However, despite the excellent performance of the hybrid decomposition-based GRU and SVM models for monthly runoff forecasting, it is necessary to address several limitations, to demonstrate the future possibilities for further study. One of the drawbacks is that the performance of the models is highly dependent on the reliability of the hydrological data, parameter selection by ML models, and the mode selection by VMD. Moreover, the two-stage decomposition approach (ICEEMDAN-VMD) produces many IMFs, due to which the implementation of these models, is a time-consuming task. Consequently, the advanced techniques are necessary for accurate hydrological runoff studies to deal with the limitations of the existing models. The authors expect that this study will provide new directions to study the runoff series forecasting, and will be beneficial for technical and scientific communities.

Conclusions

This study developed a three-stage hybrid model for the runoff forecasting of Swat river, Pakistan, by an ensemble of the ICEEMDAN-VMD decomposition techniques with the GRU algorithm. Seven other models were also developed for performance comparison by utilizing four statistical performance indices. The following can be concluded, from this study based on the results of the forecasting accuracy and the error reduction, regarding the runoff time series forecasting:

- Three-stage hybrid models (IVG, ICEEMDAN-VMD-SVM) combining a two-stage signal decomposition approach (ICEEMDAN-VMD) with ML models (GRU, SVM) perform better compared to the two-stage hybrid (ICEEMDAN-GRU, VMD-GRU, ICEEMDAN-SVM, VMD-SVM) and standalone models (GRU and SVM) in the training period. Moreover, the three-stage hybrid models also outperform in the testing period, except the VMD-GRU model, which shows better results than the ICEEMDAN-VMD-SVM model.
- IVG model outperforms all the other models in the training and testing periods, which validates the applicability of the proposed model for the runoff forecasting.
- Both the GRU and SVM techniques are feasible for the runoff forecasting, while the GRU is superior to the SVM algorithm.
- Two-stage hybrid models coupling ML models with single-stage signal decomposition techniques show better performance than the standalone models.
- Both VMD and ICEEMDAN decomposition techniques are applicable for the decomposition of runoff time series, and VMD performs better than the ICEEMDAN technique.
- Limitations: The challenge of the availability of accurate runoff data, the sensitivity of decomposition and ML models to the parameters and hyperparameters selection, and lack of the physical relations in the case of the data-driven models add complexity, in the modeling of data-driven models for the runoff forecasting.

Significance and future study: The superior forecasting results by the IVG model indicate the suitability of the IVG model for the runoff forecasting. The hybrid models combining decomposition and ML models highlight the suitability of ICEEMDAN and VMD techniques to handle the trends and noises, and the ML models are feasible for forecasting purposes. Therefore, this study will be helpful to forecast runoff in any river catchment, including the one with higher-order trends and noises. Further development in the runoff forecasting is vital considering the societal, ecological, and financial advantages of the accurate runoff forecasting. Consequently, the future study will consider novel deep learning methodologies to study the nonlinear relations between temperature, runoff, and precipitation.

Acknowledgements

This study was funded by the National Natural Science Foundation of China (Grant No. 51607105); and the Provincial Natural Science Foundation of HUBEI Province (Grant No. 2016CFA097). This financial support is gratefully appreciated and acknowledged.

The authors are also thankful to the Water and Power Authority, Pakistan, for providing data for this study.

Conflict of Interest

The authors declare no conflict of interest.

References

1. WANG H., HE K. Sensitivity Analysis of the Effects of Climate Change on Streamflow Using Climate Elasticity in the Luan River Basin, China. Pol. J. Environ. Stud., **26** (3), **2017**.
2. ZAMAN M., YUAN S., LIU J., AHMAD I., SULTAN M., QAMAR M.U., SAIFULLAH M., ADNAN M., ANJUM M.N., NAWAZ M.I. Investigating hydrological responses and adaptive operation of a hydropower station under a climate change scenario. Pol. J. Environ. Stud., **27** (5), 2337, **2018**.
3. BURGER C.M., KOLDITZ O., FOWLER H.J., BLENKINSOP S. Future climate scenarios and rainfall-runoff modelling in the Upper Gallego catchment (Spain). Environmental Pollution, **148** (3), 842, **2007**.
4. ZHOU C., SUN N., CHEN L., DING Y., ZHOU J., ZHA G., LUO G., DAI L., YANG X. Optimal Operation of Cascade Reservoirs for Flood Control of Multiple Areas Downstream: A Case Study in the Upper Yangtze River Basin. Water, **10** (9), 1250, **2018**.
5. CHEN L., SUN N., ZHOU C., ZHOU J., ZHOU Y., ZHANG J., ZHOU Q. Flood Forecasting Based on an Improved Extreme Learning Machine Model Combined with the Backtracking Search Optimization Algorithm. Water, **10** (10), 1362, **2018**.
6. REZAIE-BALF M., FANI NOWBANDEGANI S., SAMADI S.Z., FALLAH H., ALAGHMAND S. An Ensemble Decomposition-Based Artificial Intelligence Approach for Daily Streamflow Prediction. Water, **11** (4), 709, **2019**.
7. SINGH H., SANKARASUBRAMANIAN A. Systematic uncertainty reduction strategies for developing streamflow forecasts utilizing multiple climate models and hydrologic models. Water Resources Research, **50** (2), 1288, **2014**.
8. BAI Y., CHEN Z., XIE J., LI C. Daily reservoir inflow forecasting using multiscale deep feature learning with hybrid models. Journal of Hydrology, **532**, 193, **2016**.
9. CHU H., WEI J., LI J., QIAO Z., CAO J. Improved medium-and long-term runoff forecasting using a multimodel approach in the Yellow River Headwaters region based on large-scale and local-scale climate information. Water, **9** (8), 608, **2017**.
10. ADAMOWSKI J., SUN K. Development of a coupled wavelet transform and neural network method for flow forecasting of non-perennial rivers in semi-arid watersheds. Journal of Hydrology, **390** (1-2), 85, **2010**.
11. SOLOMATINE D.P. Data- driven modeling and computational intelligence methods in hydrology. Encyclopedia of hydrological sciences, **2006**.
12. SEO Y., KIM S., SINGH V. Machine learning models coupled with variational mode decomposition: A new approach for modeling daily rainfall-runoff. Atmosphere, **9** (7), 251, **2018**.
13. ABBOT J., MAROHASY J. Input selection and optimisation for monthly rainfall forecasting in Queensland, Australia, using artificial neural networks. Atmospheric Research, **138**, 166, **2014**.
14. YOON H., KIM Y., HA K., LEE S.-H., KIM G.-P. Comparative evaluation of ANN-and SVM-time series models for predicting freshwater-saltwater interface fluctuations. Water, **9** (5), 323, **2017**.
15. YASEEN Z.M., EL-SHAFIE A., JAAFAR O., AFAN H.A., SAYL K.N. Artificial intelligence based models for stream-flow forecasting: 2000–2015. Journal of Hydrology, **530**, 829, **2015**.
16. FAHIMI F., YASEEN Z.M., EL-SHAFIE A. Application of soft computing based hybrid models in hydrological variables modeling: a comprehensive review. Theoretical and Applied Climatology, **128** (3-4), 875, **2017**.
17. FOTOVATIKHAH F., HERRERA M., SHAMSHIRBAND S., CHAU K.-W., FAIZOLLAHZADEH ARDABILI S., PIRAN M.J. Survey of computational intelligence as basis to big flood management: Challenges, research directions and future work. Engineering Applications of Computational Fluid Mechanics, **12** (1), 411, **2018**.
18. ÜNEŞ F., DEMIRCI M., TAŞAR B., KAYA Y.Z., VARÇIN H. Estimating Dam Reservoir Level Fluctuations Using Data-Driven Techniques. Pol. J. Environ. Stud., **28** (5), **2019**.
19. GIZAW M.S., GAN T.Y. Regional flood frequency analysis using support vector regression under historical and future climate. Journal of Hydrology, **538**, 387, **2016**.
20. GRANATA F., GARGANO R., DE MARINIS G. Support vector regression for rainfall-runoff modeling in urban drainage: A comparison with the EPA's storm water management model. Water, **8** (3), 69, **2016**.
21. GONG Y., ZHANG Y., LAN S., WANG H. A comparative study of artificial neural networks, support vector machines and adaptive neuro fuzzy inference system for forecasting groundwater levels near Lake Okeechobee, Florida. Water Resources Management, **30** (1), 375, **2016**.
22. CHU H., WEI J., LI T., JIA K. Application of support vector regression for mid-and long-term runoff forecasting in "Yellow river headwater" region. Procedia Engineering, **154**, 1251, **2016**.
23. CARRIERE P., MOHAGHEGH S., GASKARI R. Performance of a virtual runoff hydrograph system. Journal of Water Resources Planning Management, **122** (6), 421, **1996**.
24. LIN HSU K., GUPTA H.V., SOROOSHIAN S. Application of a recurrent neural network to rainfall-runoff modeling. Proceedings of the 1997 24th Annual Water Resources Planning and Management Conference. **1997**. ASCE.
25. KRATZERT F., KLOTZ D., BRENNER C., SCHULZ K., HERRNEGGER M. Rainfall-runoff modelling using long short-term memory (LSTM) networks. Hydrology Earth System Sciences, **22** (11), 6005, **2018**.
26. RAVANELLI M., BRAKEL P., OMOLOGO M., BENGIO Y. Light gated recurrent units for speech recognition. IEEE Transactions on Emerging Topics in Computational Intelligence, **2** (2), 92, **2018**.
27. ZHOU J., LI W., YU X., XU X., YUAN X., WANG J. Elman-Based Forecaster Integrated by Adaboost Algorithm in 15 min and 24 h ahead Power Output Prediction Using PM2.5 Values, PV Module Temperature, Hours of Sunshine, and Meteorological Data. Polish Journal of Environmental Studies, **28** (3), 1999, **2019**.
28. LI W., QUAN C., WANG X., ZHANG S. Short-Term Power Load Forecasting Based on a Combination of VMD and ELM. Pol. J. Environ. Stud., **27** (5), 2143, **2018**.

29. AKRAMI S.A., ELSHAFIE A., JAAFAR O. Improving Rainfall Forecasting Efficiency Using Modified Adaptive Neuro-Fuzzy Inference System (MANFIS). Water Resources Management, **27** (9), 3507, **2013**.
30. SAHOO G.B., SCHLADOW S.G., REUTER J.E. Forecasting stream water temperature using regression analysis, artificial neural network, and chaotic non-linear dynamic models. Journal of Hydrology, **378** (34), 325, **2009**.
31. DIETTERICH T.G. Ensemble methods in machine learning. International workshop on multiple classifier systems. **2000**. Springer.
32. SAJEDI-HOSSEINI F., MALEKIAN A., CHOUBIN B., RAHMATI O., CIPULLO S., COULON F., PRADHAN B. A novel machine learning-based approach for the risk assessment of nitrate groundwater contamination. Science of the total environment, **644**, 954, **2018**.
33. MOSAVI A., OZTURK P., CHAU K.-W. Flood prediction using machine learning models: Literature review. Water, **10** (11), 1536, **2018**.
34. ZHANG J., HOU G., MA B., HUA W. Operating characteristic information extraction of flood discharge structure based on complete ensemble empirical mode decomposition with adaptive noise and permutation entropy. Journal of Vibration Control, **24** (22), 5291, **2018**.
35. OUYANG Q., LU W., XIN X., ZHANG Y., CHENG W., YU T. Monthly rainfall forecasting using EEMD-SVR based on phase-space reconstruction. Water Resources Management, **30** (7), 2311, **2016**.
36. KUMAR P., FOUFOULAGEORGIOU E. A multicomponent decomposition of spatial rainfall fields: 1. Segregation of large- and small- scale features using wavelet transforms. Water Resources Research, **29** (8), 2515, **1993**.
37. SACO P.M., KUMAR P. Coherent modes in multiscale variability of streamflow over the United States. Water Resources Research, **36** (4), 1049, **2000**.
38. SANG Y., WANG Z., LIU C. Discrete wavelet-based trend identification in hydrologic time series. Hydrological Processes, **27** (14), 2021, **2013**.
39. HEYDARI M., GHADIM H.B., RASHIDI M., NOORI M. Application of Holt-Winters Time Series Models for Predicting Climatic Parameters (Case Study: Robat Garah-Bil Station, Iran). Polish Journal of Environmental Studies, **29** (1), 617, **2019**.
40. HUANG N.E., SHEN Z., LONG S.R., WU M.C., SHIH H.H., ZHENG Q., YEN N.-C., TUNG C.C., LIU H.H. The empirical mode decomposition and the Hilbert spectrum for nonlinear and non-stationary time series analysis. Proceedings of the Royal Society of London. Series A: Mathematical, Physical and Engineering Sciences, **454** (1971), 903, **1998**.
41. WU Z., HUANG N.E. A study of the characteristics of white noise using the empirical mode decomposition method. Proceedings of the Royal Society of London. Series A: Mathematical, Physical and Engineering Sciences, **460** (2046), 1597, **2004**.
42. WU Z., HUANG N.E. Ensemble empirical mode decomposition: a noise-assisted data analysis method. Advances in Adaptive Data Analysis, **1** (01), 1, **2009**.
43. XU X., REN W. A Hybrid Model Based on a Two-Layer Decomposition Approach and an Optimized Neural Network for Chaotic Time Series Prediction. Symmetry, **11** (5), 610, **2019**.
44. LEE H.S. Improvement of Decomposing Results of Empirical Mode Decomposition and its Variations for Sea-level Records Analysis. Journal of Coastal Research, **85** (sp1), 526, **2018**.
45. COLOMINAS M.A., SCHLOTTHAUER G., TORRES M.E. Improved complete ensemble EMD: A suitable tool for biomedical signal processing. Biomedical Signal Processing and Control, **14**, 19, **2014**.
46. ZHANG J., GUO Y., SHEN Y., ZHAO D., LI M. Improved CEEMDAN – wavelet transform de-noising method and its application in well logging noise reduction. Journal of Geophysics and Engineering, **15** (3), 775, **2018**.
47. DRAGOMIRETSKIY K., ZOSSO D. Variational mode decomposition. IEEE Transactions on Signal Processing, **62** (3), 531, **2013**.
48. SHI P., YANG W. Precise feature extraction from wind turbine condition monitoring signals by using optimised variational mode decomposition. IET Renewable Power Generation, **11** (3), 245, **2016**.
49. ADNAN M., NABI G., KANG S., ZHANG G., ADNAN R.M., ANJUM M.N., IQBAL M., ALI A.F. Snowmelt Runoff Modelling under Projected Climate Change Patterns in the Gilgit River Basin of Northern Pakistan. Pol. J. Environ. Stud., **26** (3), **2017**.
50. KHAN M.I., LIU D., FU Q., FAIZ M.A. Detecting the persistence of drying trends under changing climate conditions using four meteorological drought indices. Meteorological Applications, **25** (2), 184, **2018**.
51. REHMAN H., KAMAL A. Indus Basin river system-Flooding and flood mitigation. 8th International River Symposium. **2005**.
52. HASHMI H.N., SIDDIQUI Q.T.M., GHUMMAN A.R., KAMAL M.A., MUGHAL H. A critical analysis of 2010 floods in Pakistan. African Journal of Agricultural Research, **7** (7), 1054, **2012**.
53. GRONEWOLD N. Is the flooding in Pakistan a climate change disaster. Scientific American, **18**, **2010**.
54. KHAN M.I., LIU D., FU Q., SADDIQUE Q., FAIZ M.A., LI T., QAMAR M.U., CUI S., CHENG C. Projected changes of future extreme drought events under numerous drought indices in the Heilongjiang Province of China. Water Resources Management, **31** (12), 3921, **2017**.
55. FENG Z.-K., NIU W.-J., CHENG C.-T., LUND J.R. Optimizing hydropower reservoirs operation via an orthogonal progressive optimality algorithm. Journal of Water Resources Planning and Management, **144** (3), 04018001, **2018**.
56. XU B., ZHONG P.A., ZAMBON R.C., ZHAO Y., YEH W.W.G. Scenario tree reduction in stochastic programming with recourse for hydropower operations. Water Resources Research, **51** (8), 6359, **2015**.
57. WANG W.-C., CHAU K.-W., QIU L., CHEN Y.-B. Improving forecasting accuracy of medium and long-term runoff using artificial neural network based on EEMD decomposition. Environmental research, **139**, 46, **2015**.
58. YUAN Y., TIAN C., LU X. Auxiliary loss multimodal GRU model in audio-visual speech recognition. IEEE Access, **6**, 5573, **2018**.
59. AHMAD I., TANG D., WANG T., WANG M., WAGAN B. Precipitation Trends over Time Using Mann-Kendall and Spearman's rho Tests in Swat River Basin, Pakistan. Advances in Meteorology, **2015**, 1, **2015**.
60. SATTAR H., SARWAR S., SHRESTHA S. Hydrologic Impact of Climate Change on Planned Hydro Dams in Swat River Basin. International Conference on Dam Safety Management and Engineering. **2019**. Springer.

61. SU W., LEI Z., YANG L., HU Q. Mold-level prediction for continuous casting using VMD–SVR. Metals, **9** (4), 458, **2019**.
62. NIU M., HU Y., SUN S., LIU Y. A novel hybrid decomposition-ensemble model based on VMD and HGWO for container throughput forecasting. Applied Mathematical Modelling, **57**, 163, **2018**.
63. XU J., TANG B., HE H., MAN H. Semisupervised feature selection based on relevance and redundancy criteria. IEEE transactions on neural networks, **28** (9), 1974, **2016**.
64. GAO X., LI X., ZHAO B., JI W., JING X., HE Y. Short-Term Electricity Load Forecasting Model Based on EMD-GRU with Feature Selection. Energies, **12** (6), 1140, **2019**.
65. PETNEHÁZI G. Recurrent neural networks for time series forecasting. arXiv, **2019**.
66. REN B., LIANG J., YAN B., LEI X., FU W., NI X., GUO J. Parameter Optimization of Double-Excess Runoff Generation Model. Pol. J. Environ. Stud., **27** (2), **2018**.
67. QIN J., LIANG J., CHEN T., LEI X., KANG A. Simulating and Predicting of Hydrological Time Series Based on TensorFlow Deep Learning. Pol. J. Environ. Stud., **28** (2), **2019**.
68. WANG Y., LIU M., BAO Z., ZHANG S. Short-term load forecasting with multi-source data using gated recurrent unit neural networks. Energies, **11** (5), 1138, **2018**.
69. FENG Z.-K., NIU W.-J., WANG W.-C., ZHOU J.-Z., CHENG C.-T. A mixed integer linear programming model for unit commitment of thermal plants with peak shaving operation aspect in regional power grid lack of flexible hydropower energy. Energy, **175**, 618, **2019**.
70. ZHAO T., ZHAO J., LIU P., LEI X. Evaluating the marginal utility principle for long-term hydropower scheduling. Energy Conversion and Management, **106**, 213, **2015**.
71. FENG Z.-K., NIU W.-J., CHENG C.-T., WU X.-Y. Optimization of hydropower system operation by uniform dynamic programming for dimensionality reduction. Energy, **134**, 718, **2017**.